

DOES THE EXCITATION AND DAMPING OF THE ACOUSTIC EIGENMODES VARY OVER THE SOLAR CYCLE? AN INSIGHT FROM LOI OBSERVATIONS

W. J. Chaplin¹ and T. Appourchaux²

¹School of Physics and Astronomy, University of Birmingham, Edgbaston, Birmingham, B15 2TT, U.K.

²Solar System Division, Space Science Dept., ESA/ESTEC, 2200 AG Noordwijk, The Netherlands

ABSTRACT

We have used observations made by the LOI instrument on board the ESA/NASA SOHO satellite in order to try and uncover variations in the excitation and damping of the low-angular-degree solar acoustic eigenmodes over the solar cycle. These data were collected on the rising phase of activity cycle 23. We have divided the dataset into independent 136-d and 1-yr time series and fitted the modes in the complex Fourier (frequency) domain to yield estimates of the line widths and amplitudes of the modes. The extracted parameters have then been analyzed in order to search for solar-cycle-induced variations.

Over the range $2600 \leq \nu \leq 3600 \mu\text{Hz}$, we uncover a mean implied activity minimum-to-maximum increase in the frequency-domain line widths of 21 ± 3 per cent; a mean decrease of 37 ± 3 per cent decrease in the mode heights; and a mean decrease of 18 ± 4 per cent in the mode powers. Our analysis indicates that – at the level of precision of the available data – the rate at which energy is supplied to the modes remains constant (uncovered variation 3 ± 5 per cent). These results are in reasonable agreement with recent claims by Chaplin et al. (2000) and Komm, Howe and Hill (2000) from analyses of BiSON and GONG data respectively. Furthermore, the signs and relative magnitudes of the extracted changes are consistent with the speculation made by Chaplin et al. that it is alterations in the damping, and not the forcing, of the modes that gives rise to the variations observed over the solar activity cycle.

Key words: Sun: activity – Sun: oscillations.

1. INTRODUCTION

Observations of variations in the eigenfrequencies of the acoustic mode vibrations of the Sun that are correlated with the solar activity cycle are now well documented, e.g., at low and intermediate angular degrees (Woodard & Noyes 1985; Elsworth et al. 1990,

1994; Anguera Gubau et al. 1992; Regulo et al. 1994; Chaplin et al. 1998; Jimenez-Reyes et al. 1998; and Libbrecht & Woodard 1990; Woodard et al. 1991; Bachmann & Brown 1993; Rhodes Jr et al. 1993; Howe, Komm & Hill 1999; Bhatnager, Jain & Tripathy 1999; Dziembowski et al. 2000). Attempts to uncover changes to those mode parameters in which the excitation and damping phenomenology of the modes is coded have proved far more elusive. This is due in large part to the lower precision with which the frequency-domain modal line widths and amplitudes can be determined, but also illustrates the difficulties associated with extracting robust, unbiased estimates of these parameters.

Studies in the literature have shown evidence for a decrease in the amplitudes of the acoustic modes with increasing solar activity (e.g., Palle et al. 1990a; Anguera-Gubau et al. 1992; Elsworth et al. 1993); however, the line width parameter is more difficult to extract reliably, and this has been reflected in a series of marginally significant and sometimes contradictory claims (Palle et al. 1990b; Jefferies et al. 1990; Jefferies et al. 1993; Meunier 1997). The advent of more extensive and precise observational datasets, coupled with the use of more involved techniques of analysis, has recently led to two independent claims of line width changes by Chaplin et al. (1999) and Komm, Howe & Hill (1999) that are each highly significant and both fairly consistent. Each paper reports an increase in line width between solar minimum and maximum, in addition to a decrease in mode power, the former from an analysis of low-angular-degree (low- l) data collected by the ground-based Birmingham Solar-Oscillations Network (BiSON); and the latter from a more extensive intermediate-degree set of observations made by the Global Oscillations Network Group (GONG).

Here, we seek to uncover similar changes in another set of independent helioseismic observations made by the VIRGO/LOI instrument on board the ESA/NASA SOHO satellite. LOI observes intensity perturbations in the continuum at 500 nm, as opposed to the Doppler velocity variations observed by BiSON and GONG. Therefore, an analysis of the LOI data promises potential new information, in ad-

dition to offering further, independent confirmation of these results.

2. EXCITATION AND DAMPING PHENOMENOLOGY

A useful analogy for the p-modes is a forced, damped harmonic oscillator, of the form:

$$\frac{d^2}{dt^2}x(t) + 2\eta\frac{d}{dt}x(t) + \omega_0^2x(t) = f(t).$$

In the above: $x(t)$ is the displacement of the oscillator; ω_0 is its natural angular frequency; η is the damping constant; and $f(t)$ is the forcing function. The Fourier transform of the oscillator equation gives the shape of the expected power spectrum of the velocity signal in the vicinity of the resonance ($\omega \approx \omega_0$), i.e.,

$$\mathcal{X}(\omega) \approx \frac{\mathcal{F}(\omega)}{4\omega_0^2} \cdot \frac{1}{(\omega - \omega_0)^2 + \eta^2}, \quad (1)$$

under the assumption that $\mathcal{F}(\omega)$ – the frequency spectrum of $f(t)$ – is a slowly-varying function of ω , and $\eta \ll \omega_0$. This is essentially a Lorentzian profile, with a radian FWHM of:

$$\Delta\nu = 2\eta. \quad (2)$$

The peak height is:

$$H = \frac{\mathcal{F}(\omega)}{4\omega_0^2\eta^2}. \quad (3)$$

The power of a given mode is proportional to width times peak height, i.e.,

$$P = \pi \frac{\mathcal{F}(\omega)}{4\omega_0^2\eta}. \quad (4)$$

To a good approximation, the solar acoustic spectrum should be represented by an ensemble of such oscillators. The energy (kinetic plus potential) of a mode with associated inertia M is given by:

$$E = Mv^2 = M\beta_{I-V}^2P. \quad (5)$$

Here, v is the velocity associated with the mode, and β_{I-V} relates the intensity and velocity perturbations associated with the mode.

The rate at which energy is supplied to the modes, dE/dt , can be derived as follows. The energy of a damped-oscillator can be expressed as:

$$E = [\text{constant}] \times A^2 = [\text{constant}] \times e^{-2\eta t},$$

where A is the amplitude of the motion. It follows that:

$$\log E = -2\eta t + \log[\text{constant}],$$

and taking derivatives:

$$dE/dt = -2\eta E. \quad (6)$$

If we combine Equations 4, 5 and 6, we have:

$$dE/dt = \dot{E} = -\pi\beta_{I-V}^2 \frac{\mathcal{F}(\omega)M}{2\omega_0^2}. \quad (7)$$

The oscillator analogy therefore tells us that observations of the modal line widths, $\Delta\nu$, might be expected to give a direct measure of the damping rate, η ; the velocity power, P , in the modes reflects the balance between the excitation – as expressed by $\mathcal{F}(\omega)$ – and the damping; while the energy supply rate, \dot{E} , provides information regarding the forcing function, $\mathcal{F}(\omega)$. At this point we note that $\Delta\nu$ and \dot{E} are independent of one another.

We assume for the purposes of the following discussion that changes to ω and M over the activity cycle can be ignored, since the magnitudes of these variations are smaller than the uncertainties associated with the extracted height and width parameters in the LOI data (see Chaplin et al. 1999 for a thorough discussion of this point). Then, using the equations above, we can relate how variations in η and $\mathcal{F}(\omega)$ propagate as changes in the ‘observables’, $\Delta\nu$, H , P , E and \dot{E} :

$$\frac{\delta\Delta\nu}{\Delta\nu} = \frac{\delta\eta}{\eta}, \quad (8)$$

$$\frac{\delta H}{H} = \frac{\delta\mathcal{F}}{\mathcal{F}} - 2\frac{\delta\eta}{\eta}, \quad (9)$$

$$\frac{\delta P}{P} = \frac{\delta\mathcal{F}}{\mathcal{F}} - \frac{\delta\eta}{\eta}, \quad (10)$$

and

$$\frac{\delta\dot{E}}{\dot{E}} = \frac{\delta\mathcal{F}}{\mathcal{F}}. \quad (11)$$

These expressions indicate that changes to the observed velocity power and energy will result from changes to the damping rate, regardless of variations in the forcing; the energy supply rate remains fixed, since it is independent of the damping. Changes to the forcing alone will give rise to variations in the modal powers, energies and energy supply rates, while the line widths remain unaltered.

We now seek to extract – and then interpret – variations in the observables introduced above from an analysis of several LOI power spectra which span a substantial portion of the rising phase of activity cycle 23.

3. DATA AND ANALYSIS

The LOI dataset – which spans the period 1996 March through 2000 April – has been divided into nine 136-d and four 1-yr segments. The range of solar activity levels covered by these data is indicated in Figure 1, where we show the variation of the 10.7-cm radio flux (in RF units, smoothed with a 1-yr filter) during the previous (cycle number 22) and

current (number 23) activity cycles. The period covered by the LOI data analyzed here is rendered with a thick line.

Each complex Fourier (frequency) spectrum was fitted to yield estimates of the modal parameters for $1 \leq l \leq 3$ (see Appourchaux, Rabello-Soares & Gizon 1998 for a full discussion of the technique). The individual components of a given multiplet were constrained to have the same width. However, we fitted separate heights at each m . The fitted height parameters used in the analysis are a weighted average over all components (i.e., from $-m \leq l \leq m$).

The fitting extracts estimates of the natural logarithms of the frequency-domain mode widths and widths (see Toutain & Appourchaux 1994; Chaplin et al. 1999). Extracted solar-cycle variations in the log-width, $w(l, n)$, and log-height, $h(l, n)$, therefore correspond to fractional variations in the absolute parameters, $\Delta\nu(l, n)$ and $H(l, n)$ respectively.

The logarithm of the intensity power in mode is given by:

$$p(l, n) = w(l, n) + h(l, n) + \beta_{\text{cal}}, \quad (12)$$

Here, $h(l, n)$ now describes the weighted average over all fitted height components at the identified (l, n) . The factor k_{cal} provides a proper calibration of the power (this non-trivial issue is dealt with at great length in Appourchaux et al. 2000). With reference to Equations 5 and 6, the natural logarithms of the energy and energy supply rates are given by:

$$e(l, n) = w(l, n) + \varrho(l, n) + h(l, n) + \beta_{\text{cal}}, \quad (13)$$

and

$$\dot{e}(l, n) = 2w(l, n) + \varrho(l, n) + h(l, n) + \beta_{\text{cal}} + \beta_{\dot{e}} \quad (14)$$

where $\varrho(l, n)$ is the logarithm of the associated modal mass, and $\beta_{\dot{e}}$ gives a proper calibration of \dot{e} . Since we are performing a differential analysis of the mode parameters, $\varrho(l, n)$, β_{cal} and $\beta_{\dot{e}}$ – which we assume remain constant over time – can all be ignored.

Owing to the fact there is a strong degree of correlation between the estimates of the heights and widths extracted by the fitting procedure, the propagation of errors must reflect this when the uncertainties in $p(l, n)$, $e(l, n)$ and $\dot{e}(l, n)$ are determined. Take, for example, the calculation of the uncertainty in $p(l, n)$: if $\sigma_{w(l, n)}$ and $\sigma_{h(l, n)}$ are the uncertainties in $w(l, n)$ and $h(l, n)$ respectively, then the usual combination-of-errors formula must be modified according to:

$$\sigma_{p(l, n)}^2 = \sigma_{w(l, n)}^2 + \sigma_{h(l, n)}^2 - 2|\rho(w, h)| \cdot \sigma_{w(l, n)} \cdot \sigma_{h(l, n)}, \quad (15)$$

where the correlation coefficient between the height and width parameters, $\rho(w, h)$, was estimated to be ~ -0.9 (over the range of modes fitted here) from extensive Monte Carlo simulations.

Our fitting procedures provided us with estimates of $w(l, n)$ and $h(l, n)$ for the modes in each spectrum; a

little rudimentary analysis then yielded estimates of $p(l, n)$, $e(l, n)$ and $\dot{e}(l, n)$. For each of the resulting 136-d and 1-yr grand datasets (the two time bases were treated separately) we selected a subset of spectra that were made from data collected at low levels of solar activity. To do this, we used the 10.7-cm radio flux – averaged over the duration of each time series – as our proxy of the level of activity. Each of the logarithmic parameters from these data were then averaged at each (n, l) to yield mean estimates of the parameters at low activity. These then served as a reference against which to compute variations (residuals) for all spectra. We then carried out a linear regression of each set of parameter residuals in adjacent segments in frequency space with the 10.7-cm radio flux (averaged over the duration of the time series of each spectrum). From the extracted gradient of the regression, we could then infer from the variation of the radio flux the total mean fractional change in the parameter from activity minimum to maximum over the considered bandwidth (i.e., over those modes used in the regression). At each stage of the analysis, we made use of the rejection algorithms developed by Chaplin et al. (1998) to treat outliers in the data.

4. RESULTS AND DISCUSSION

In Figure 2, we show the results of analyzing the nine 136-d spectra. Displayed are the absolute shifts of the natural logarithms of the mode widths (upper two panels) and heights (lower panels), averaged over all fitted modes in the range $2900 \leq \nu \leq 3400 \mu\text{Hz}$. Each plotted datum corresponds to a fractional variation of the absolute parameter. The left-hand panels show the mean shifts for each spectrum as a function of the 10.7-cm flux measured averaged over the duration of each time series. The solid line in each panel is a linear fit to the activity measure. The shifts are rendered as a function of epoch in the right-hand panels (with the solid lines showing the prediction of the best linear fits shown in the left-hand panels). The plotted error bars correspond to 1σ uncertainties

These data reveal a clear increase in line width and decrease in height with increasing solar activity. In Figure 3 we plot the absolute differences of the natural logarithms of the mode widths (left-hand panel) and heights (right-hand panel) between two 1-yr spectra as a function of frequency. The spectra were generated from observations made between 1996 March and 1997 March (i.e., at low activity); and between 1999 March and 2000 March (i.e., at higher levels of activity) respectively. The mean 10.7-cm flux level increased from ~ 70 RF units in the first set to ~ 158 RF units in the latter. As a result of applying a 1-yr smoothing filter to the daily record of the radio flux, we estimate that the peak 1-yr-mean level of activity might be expected to reach ~ 210 RF units although of course we note that the precise value changes from cycle to cycle. The value

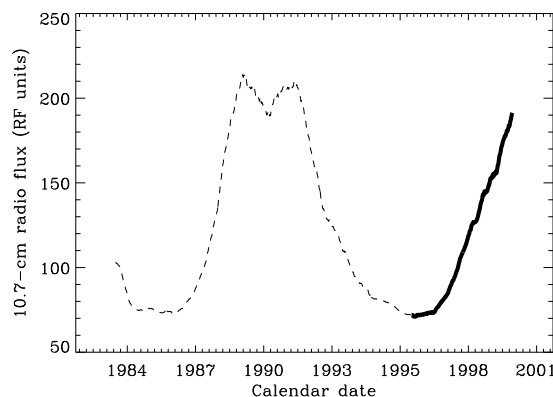


Figure 1. Variation of the 10.7-cm radio flux (in RF units, smoothed with a 1-yr filter) during the previous (cycle number 22) and current (number 23) solar activity cycles. The period covered by the LOI data is rendered with a thick line.

quoted here does nevertheless serve as a useful guide, and we also use it to extrapolate the extracted shifts to those expected for the full, minimum-to-maximum swing of the cycle.

Table 1 presents the implied fractional full-swing shifts for the various mode parameters, averaged over all modes in the range $2600 \leq \nu \leq 3600 \mu\text{Hz}$. These data were extracted from an analysis of the more-precise 1-yr dataset. We recall the equations given in Section 2. The extracted increase in the widths clearly implies a net increase in the damping rate, η , with activity (cf. Equation 2). The energy supply rate is independent of η , and gives information regarding the forcing, $\mathcal{F}(\omega)$ (Equation 7). The results in Table 1 imply that – at the level of precision of the data – $\mathcal{F}(\omega)$ can be considered to remain constant over the solar cycle. With reference to Equations 8 through 11, changes to the mode heights and powers would then be expected to arise solely from variations in the damping parameter, η . The observed changes should then satisfy:

$$\frac{\delta\Delta\nu}{\Delta\nu} = \frac{\delta\eta}{\eta} = -1/2 \frac{\delta H}{H} = -\frac{\delta P}{P}.$$

Within errors, this is what we find in Table 1.

The frequency range used here matches that considered by Chaplin et al. (2000), who analyzed low- l BiSON data collected on the falling phase of cycle 22 (between 1991 and 1997). They uncovered mean, fractional activity minimum-to-maximum variations of: 24 ± 3 per cent in mode line width; -46 ± 5 per cent in mode height; -22 ± 3 per cent in mode power; and a 0 ± 4 per cent change in the energy supply rate. The results extracted from our analysis of the LOI data are in good agreement with the BiSON values.

Komm, Howe & Hill (2000) analyzed GONG data (up to $l = 150$) collected between 1995 May and 1998 October, i.e., on the first half of the activity rise of cycle 23. They also uncovered an increase in line width and decrease in height and power at higher

levels of activity. Furthermore, their analysis strongly suggests that the shifts may increase in strength when $l < 50$; above this, the observed changes would appear to be invariant of l .

Their results imply (with some extrapolation) an approximate low- l activity minimum-to-maximum fractional increase of ≈ 17 per cent in line width; a ≈ 38 per cent decrease in height; and a ≈ 29 per cent decrease in power. When their results are averaged over the complete angular degree range covered (up to $l = 150$, but with sparse coverage below $l = 5$) and $2700 \leq \nu \leq 3300 \mu\text{Hz}$ the implied changes are ~ 10 per cent in line width; in height, roughly ~ -13 per cent at $|m/l| = 0$ and ~ 25 per cent at $|m/l| = 1$; and in power, roughly ~ 14 per cent at $|m/l| = 0$ and ~ 20 per cent at $|m/l| = 1$.

The GONG ‘low- l ’ values are in reasonable agreement with our results, although the relative sizes of the observed variations do differ from those extracted from the BiSON and LOI data, i.e., if we are guided by the oscillator analogy, they imply that changes to the forcing (and not just the damping) must take place. There are also differences in the results that depend upon the azimuthal order – and hence the spatial structure – of the modes. These should be borne in mind when comparisons are made with the BiSON results, that will tend to reflect the behaviour of the $|m/l| = 1$ components, to which full-disc observations are most sensitive, and the LOI results, which we quote here as a weighted average over all m . A preliminary analysis as a function of $|m/l|$ failed to uncover any significant change in behaviour over the restricted range in l considered.

Komm, Howe & Hill also found that the variations in width and power appear to be peaked at frequencies of $\sim 3000 \mu\text{Hz}$. Chaplin et al. drew attention to the presence of possible similar behaviour in their data, but noted that the formal significance of the effect was probably marginal at best. Here, a visual inspection of the shifts plotted in Figure 3 may also hint at a similar frequency dependence. However, we

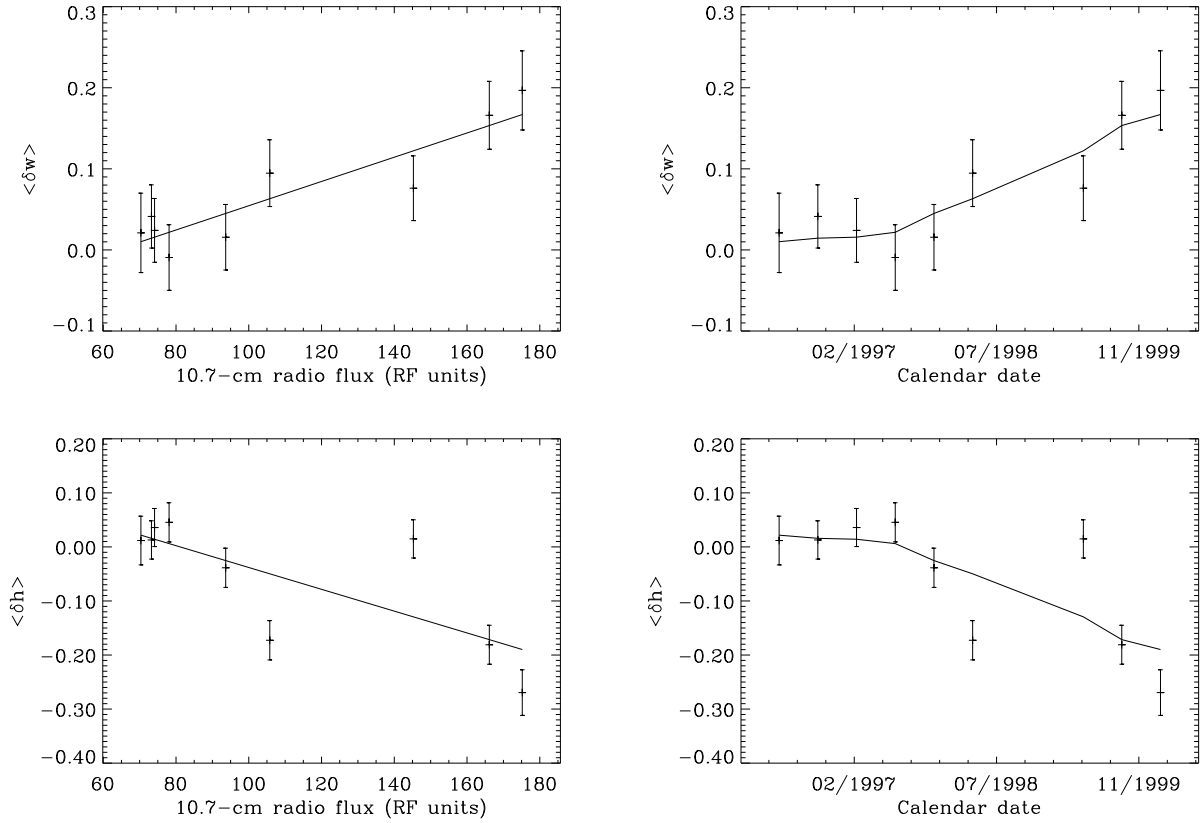


Figure 2. Results of analyzing the 136-d spectra for solar-cycle changes in the width and height parameters. Plotted are the absolute shifts of natural logarithms of the mode widths (upper two panels) and heights (lower panels), averaged over all fitted modes in the range $2900 \leq \nu \leq 3400 \mu\text{Hz}$. Each datum corresponds to a fractional variation of the absolute parameter. Left-hand panels – the mean shifts for each spectrum, plotted as a function of the mean 10.7-cm flux measured over the duration of each time series. The solid line in each panel is the linear fit to the activity measure. Right-hand panels – the mean shifts, now rendered as a function of epoch. The solid line corresponds to the best-fit prediction (i.e., from the linear fit in the left-hand panels). The plotted error bars in each panel correspond to 1σ uncertainties.

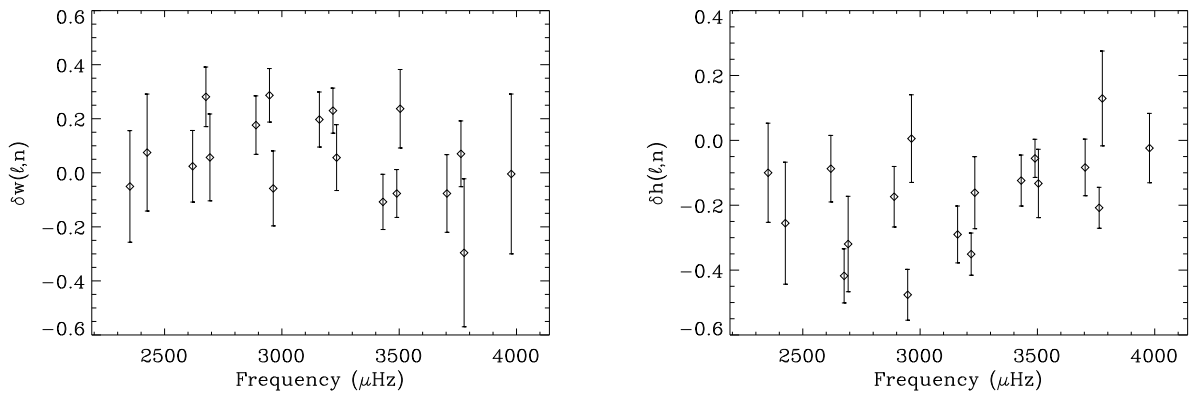


Figure 3. The absolute differences of the natural logarithms of the mode widths (left-hand panel) and heights (right-hand panel) between two 1-yr spectra, as a function of frequency. The spectra were generated from observations made between 1996 March and 1997 March (i.e., at low activity); and between 1999 March and 1999 March (i.e., at higher levels of activity) respectively. Each datum corresponds to a fractional variation of the absolute parameter.

Table 1. Mean, variations over the solar cycle (those implied for the full minimum-to-maximum activity swing) of several *p*-mode parameters – averaged over modes in the range $2600 \leq \nu \leq 3600 \mu\text{Hz}$ – as inferred from the analysis of the 1-yr LOI spectra.

<i>Parameter</i>	<i>Mean, fractional change (per cent)</i>
Line width	21 ± 3
Peak height	-37 ± 3
Velocity power	-18 ± 4
Energy supply rate	3 ± 5

draw to the attention of the reader the lengthy discussion by Chaplin et al. regarding sources of bias in results of this type, particularly those relevant at low and high frequencies. The apparent reduction in the size of the shifts at the extreme ends of Figure 3 may simply reflect bias in the estimated mean variations that arises when the signal-to-noise ratio in the modes is reduced. We are currently investigating further with a series of intensive Monte Carlo simulations.

ACKNOWLEDGMENTS

This work utilizes data collected by the VIRGO instrument on board the SOHO satellite, and the ground-based Birmingham Solar-Oscillations Network (BiSON). We would like to thank the members of both teams for allowing us to use these data. SOHO is a project of international cooperation between ESA and NASA. BiSON is funded by the UK Particle Physics and Astronomy Research Council.

REFERENCES

- Anguera Gubau M., Palte P. L., Perez Hernandez F., Regulo C., Roca Cortes T., 1992, *A&A*, 255, 363
- Appourchaux T., Gizon L. & Rabello-Soares M. C., 1998, *A&AS*, 132, 107
- Appourchaux T., Fröhlich C., Anderson B., Appourchaux T., Berthomieu G., Chaplin W. J., Elsworth Y., Finsterle W., Gough D. O., Hoeksema J. T., Isaak G. R., Kosovichev A., Provost J., Scherrer P., Sekii T. & Toutain T., 2000, *ApJ*, 538, 401
- Bachmann K. T., Brown T. M., 1993, *ApJ*, 411, L45
- Bhatnagar A., Jain K., Tripathy S. C., 1999, *ApJ*, 521, 885
- Chaplin W. J., Elsworth Y., Isaak G. R., Lines R., McLeod C. P., Miller B. A., New R., 1998, *MNRAS*, 300, 1077
- Chaplin W. J., Elsworth Y., Isaak G. R., Miller B. A., New R., 2000, *MNRAS*, 313, 32
- Dziembowski W. A., Goode P. R., Kosovichev A. G., Schou J., 2000, *ApJ*, 537, 1026
- Elsworth Y., Howe R., Isaak G. R., McLeod C. P., & New R., 1990, *Nature*, 345, 322
- Elsworth Y., Howe R., Isaak G. R., McLeod C. P., Miller B. A., New R., Speake C. C., Wheeler S. J., 1993, *MNRAS*, 265, 888
- Elsworth Y., Howe R., Isaak G. R., McLeod C. P., Miller B. A., New R., Speake C. C. & Wheeler S. J., 1994, *ApJ*, 434, 801
- Howe R., Komm R. W., Hill F., 1999, *ApJ*, 524, 1084
- Jefferies S. M., Duvall T. L. Jr., Harvey J. W., Pomerantz M. A., 1990, in: *Progress of Seismology of the Sun and Stars*, p. 135, eds. Osaki Y., Shibahashi H., Springer-Verlag, Berlin
- Jefferies S. M., Duvall T. L. Jr., Harvey J. W., Osaki Y., Pomerantz M. A., 1993, *ApJ*, 377, 330
- Jimenez-Reyes S. J., Regulo C., Palte P. L., Roca Cortes T., 1998, *A&A*, 329, 1119
- Komm R. W., Howe R., Hill F., 2000, *ApJ*, 531, 1094
- Libbrecht K. G., Woodard M. F., 1990, *Nature*, 345, 779
- Meunier N., 1997, PhD thesis, Université D. Diderot
- Nigam R. & Kosovichev A. G., 1998, *ApJ*, 505, L51
- Palte P. L., Regulo C., Roca Cortes T., 1990a, in: *Progress of Seismology of the Sun and Stars*, p. 129, eds. Osaki Y., Shibahashi H., Springer-Verlag, Berlin
- Palte P. L., Regulo C., Roca Cortes T., 1990b, in: *Progress of Seismology of the Sun and Stars*, p. 189, eds. Osaki Y., Shibahashi H., Springer-Verlag, Berlin
- Regulo C., Jimenez A., Palte P. L., Hernandez F. P. & Cortes T. R., 1994, *ApJ*, 434, 384
- Rhodes E. J. Jr., Cacciani A., Korzennik S. G., Ulrich R. K., 1993, *ApJ*, 406, 714
- Toutain T., Appourchaux T., 1994, *A&A*, 289, 649
- Woodard M. F., Noyes R. W., 1985, *Nature*, 318, 449
- Woodard M. F., Libbrecht K. G., Kuhn J. R., Murray N., 1991, *ApJ*, 373, L81